

# Pathological Evaluation by Microtomography of Ranula. Clinical Case Report

## Evaluación Patológica por Microtomografía de Ránula. Reporte de Caso Clínico

Ellen dos Santos<sup>1</sup>; Walas Cazassa Vieira<sup>1</sup> & Fabiano Luiz Heggendorn<sup>2</sup>

DOS SANTOS, E.; VIEIRA, W. C. & HEGGENDORN, F. L. Pathological evaluation by microtomography of ranula - clinical case report. *Int. J. Odontostomat.*, 16(2):214-221, 2022.

**ABSTRACT:** This study aims to demonstrate, through a clinical case report, the applicability of the use of microtomography ( $\mu$ CT) in the histopathological evaluation of a ranula lesion on the oral floor and to evaluate the use of 2 % elemental iodine solution as a contrast agent, in order to obtain a better contrast effect in a tissue sample, thus facilitating the identification of anatomical structures, the histomorphological evaluation and the potential use of  $\mu$ CT in the imaging diagnosis of lesions. Different parameters were evaluated for obtaining images in SkyScan 1172, in a biopsied piece, when impregnated in a 10 % formalin solution and in a 2 % elemental iodine solution, when impregnated for 24h and 48h. Contrast agent impregnation was evaluated using the Hounsfield unit. The use of  $\mu$ CT allowed the identification of sialoliths dispersed inside the biopsy specimen, while the impregnation with Elemental iodine 2 % for 24h resulted in a better contrast when compared to the other conditions. The use of the Hounsfield unit allowed an adequate evaluation of the contrast obtained when the different parameters of impregnation and image acquisition were applied. The comparison between the 3D images with and without a specific marker highlighted a better evidencing of the soft tissues, with an improvement in the contrast of the images, also allowing the identification of the glandular duct obstructed by the sialoliths, allowing a conclusive histopathological evaluation of the biopsied lesion.

**KEY WORDS:** ranula, X-ray microtomography, impregnation.

## INTRODUCTION

Ránula, whose appearance resembles the belly of a frog (Mizuno & Yamaguchi, 1993), originates from the Latin word rana, from frog. This pathology is characterized by the fluctuating volume increase, having a translucent color, bluish when superficial, due to the capillaries, or normochromic, when deep. It is presented painlessly, with firm or flaccid consistency, sessile or pedunculated base, unilateral and benign (Gomes *et al.*, 2019).

Generally, the sublingual Ránula presents itself in the region of the floor of the mouth, but there is a type of clinical variation called cervical or plunging, where the extravasation of mucus occurs through the mylohyoid muscle, thus causing edema inside the neck associated or not with an increase in volume in the floor of the mouth (Neville *et al.*, 2016).

Among the etiological causes found for its occurrence, we can report traumatic episodes in the salivary gland, rupture of its duct or even obstruction by sialoliths in the salivary duct. Sialoliths are salivary stones formed and deposited inside the salivary duct or salivary gland, most commonly in the Submandibular Gland (83 to 94 %), due to the course of the Wharton Duct also for its mixed salivation (mucous and serous) (Manzi *et al.*, 2010). In the event of a total obstruction, a sialolithiasis develops, presenting regional inflammation, edema and pain at the time of mastication due to stimulation of salivary production (Manzi *et al.*, 2010).

Complementary tests, such as radiographs, ultrasound, cytology through aspiration and fine needle aspiration (Gomes *et al.*, 2019), sialography,

<sup>1</sup> Faculty of Dentistry, Universidade do Grande Rio (UNIGRANRIO), Rua Prof. José de Souza Herdy, Duque de Caxias, Rio de Janeiro, Brazil.

<sup>2</sup> Postgraduate Program in Dentistry, University of Grande Rio (UNIGRANRIO), Rua Prof. José de Souza Herdy, Duque de Caxias, Rio de Janeiro, Brazil.

scintigraphy, sialendoscopy, magnetic resonance imaging and computed tomography (Manzi *et al.*, 2010), help in the diagnosis and contribute to perform the most appropriate form of treatment for this pathology. However, for the histopathological evaluation of this lesion it is still through histology, being the gold standard, with eosin and hematoxylin stains. Here we contribute to the possibility of carrying out a histopathological evaluation of this lesion using a non-destructive method of the sample, through Computed Microtomography ( $\mu$ CT).

According to Queiroz *et al.* (2019), in the last twenty years,  $\mu$ CT has been used in pre-clinical and experimental research in multiple areas, such as geology, building materials and even in dental studies. Its use allows a non-destructive 3D analysis of the material, achieving sharpness and contrast in high resolution, through its isotropic voxels, which in volume are approximately one million times smaller than computed tomography (CT), thus allowing, perform volumetric analyses, tissue visualization and visualization of the internal area of the material to be analyzed. In the same line of reasoning, Peyrin *et al.* (2014) reported the relevance of  $\mu$ CT in their studies with trabecular bone, describing the importance attributed to the fact that this resource does not destroy the sample and can also be referred to other methodological analyses, such as histopathological analysis. The same authors also pointed out the existence of different systems, with different parameters of x-rays, and that an adequate spatial resolution is essential to obtain satisfactory images of certain specific structures.

The use of contrast in samples visualized in  $\mu$ CT was first performed by Metscher (2009), who used Lugol's iodine to monitor the embryonic development of soft tissue structures, aiming to obtain a contrast effect on the images. The low x-ray attenuation of  $\mu$ CT in soft tissues can be overcome by the development of different staining techniques (Heimel *et al.*, 2019). X-ray absorption by contrast agents, dyes of high atomic number elements, allows 3D visualization of soft tissue microstructures (Heimel *et al.*, 2019).

Different contrasts are reported, such as suspensions of barium sulfate, gallocyanin-chromalum, gold, iodine, potassium iodide, iodine, lugol's iodine, osmium tetroxide, iron oxide, lead, mercury chloride, osmium, phosphomolybdic acid, phosphotungstic, platinum, iodide potassium, silver, uranyl acetate, potassium dichromate and silver nitrate. Each of these

agents allows the visualization of a particular type of tissue and cellular structure (Orhan, 2020).

This study aims to demonstrate, through a clinical case report, the applicability of the use of  $\mu$ CT in the histopathological evaluation of a Ranula lesion on the oral floor and to evaluate the use of 2 % elemental iodine solution as a contrast agent, in order to obtain a better contrast effect in a tissue sample, thus facilitating the identification of anatomical structures, the histomorphological evaluation and the potential of the use of  $\mu$ CT in the imaging diagnosis of lesions.

## CASE REPORT

Female patient, 44 years old, attended the integrated adult clinic of the University of Grande Rio, UNIGRANRIO, reporting a transient increase in volume in the mouth floor near the region of tooth 36, with a history of development 34 days after a procedure surgical extraction of the dental element 37. Clinically, the lesion presented a floating, bullous and normochromic aspect. The occlusal and panoramic radiographic evaluation did not reveal the presence of sialolith in the region. Even without the identification of the presence of sialolith, draining of the lesion was performed with the aim of unblocking the salivary duct, without success. The patient was informed about the study, allowing his/her inclusion in the research by signing the informed consent form.

After two months of follow-up, local anesthesia was administered followed by a circular incision on the periphery of the lesion in order to perform an excisional biopsy, completely removing the lesion. The surgery was completed with several simple sutures and the biopsied material was placed in a 10 % formalin solution. After 15 days, the patient was reassessed, with no history of lesion recurrence.

**Microtomographic analysis.** The biopsied material was kept in 10 % formaldehyde solution until the images were acquired using the SkyScan 1172 microtomograph (Bruker-mCT, Kontich, Belgium). At this stage, no contrast agent was used.

The common parameters used in the acquisition of  $\mu$ CT images, at all stages, were: voltage 50Kvp; Source Current 800 mA and flat-field correction. The parameters used in this first image acquisition were shown in Table I.

Table I. Parameters for image acquisition in the different stages of histomorphological and histopathological evaluation.

Image Acquisition	First Acquisition No agent Contrasting	Second Acquisition With agent Contrasting	Third Acquisition with agent Contrasting
Aluminum Filter (Al)	Filter - Al 0,25	Filter - Al 0,25	Filter- Al 0,0
Image Pixel Size (µm)	9.33	9.33	11,46
Exposure (ms)	4000	5200	5200
Rotation Step (deg)	0,6	0,5	0,5
Frame Averaging	3	3	3

In the second image acquisition, a contrast agent was used. The tissue fragment was immersed in 2 % elemental iodine solution for 24 hours, then removed for image acquisition. The parameters used were the same as in the step above, differing in the increase in exposure and in the reduction of Rotation step (Table I).

In the third image acquisition, with the same contrast agent, the same impregnation cycle was repeated for another 24 hours, then removed for image acquisition. The parameters used were the same as in the step above, differing in the increase in Image Pixel Size and in the absence of an aluminum filter (Table I).

The images obtained from the µCT were reconstructed and processed using the NRecon program (SkyScan, Kontich, Belgium), with the following parameters: Ring artifacts reduction 7, Beam-hardening correction 46 %, Smoothing Kernel Gaussian and Defect pixel masking 50 %. During the reconstructions, the only parameter that differed was the Misalignment Compensation, being: -13.5; -20.5 and -1.0 for the first, second and third reconstruction respectively.

Then these reconstructed images were analyzed in the Data Viewer program (SkyScan, Kontich, Belgium), for visualization and evaluation in 2D of the coronal, transverse and sagittal axes, using the Hounsfield Unit (HU) as an image unit in order to evaluate the pixel intensity of artifacts found in the anatomical piece, such as sialoliths present in such lesions. Differentiating between calcified and tissue artifacts using HU.

The images were also analyzed using the CTan program (SkyScan, Kontich, Belgium) where the region of interest (ROI) was drawn, delimiting the sample, following the process of thresholding and binarization of the images, adjusting the histogram to evidence the artifacts suggestive of sialolithiasis, allowing its identification. Ultimately the 3D images were still visually evaluated in the CtVox software (SkyScan, Kontich, Belgium).

## RESULTS

The histomorphological analysis of the lesion biopsied using the µCT revealed the presence of sialoliths scattered inside the biopsy specimen in all the methodological variations for the analyses, such finding allowed the histopathological evaluation of the lesion with a conclusive diagnosis of the Ranula lesion.

The sialoliths were grouped in different regions, suggesting in some sections a straight path of the glandular duct, as shown in Figure 1 (A and B). When impregnated with a 2 % Elemental Iodine solution for 24h, using an Al 0.25 filter, it was possible to identify the path of the glandular duct connecting with the salivary gland (Figs. 2 A and B), evidencing better tissue contrast when compared to analysis without the use of a contrast agent.

The reduction of the aluminum filter in the image acquisition, Al 0.0 filter, in the biopsy specimen, in the second moment of impregnation in 2 % Elemental Iodine solution, suggested a lower contrast in the tissues, in addition to the occurrence of a loss in the signal-to- image noise.

The use of the Hounsfield Unit evidenced the difference in intensity in HU between the areas of sialoliths and the surrounding tissues. The graphical representation of the areas corresponding to the sialoliths was between 1800 and 2600 HU while the surrounding tissues were between 1000 and 1400 HU. After the use of the contrast agent, the HU values increased, due to the impregnation in the whole biopsy specimen by a contrasting agent, being between 14000 and 11000 HU for the area suggestive of sialoliths, while the surrounding areas of tissue were between 8000 and 2000 HU (Fig. 2 A.2 and B.2).

On the other hand, the reduction of the aluminum filter in the image acquisition, Al 0.0 filter,

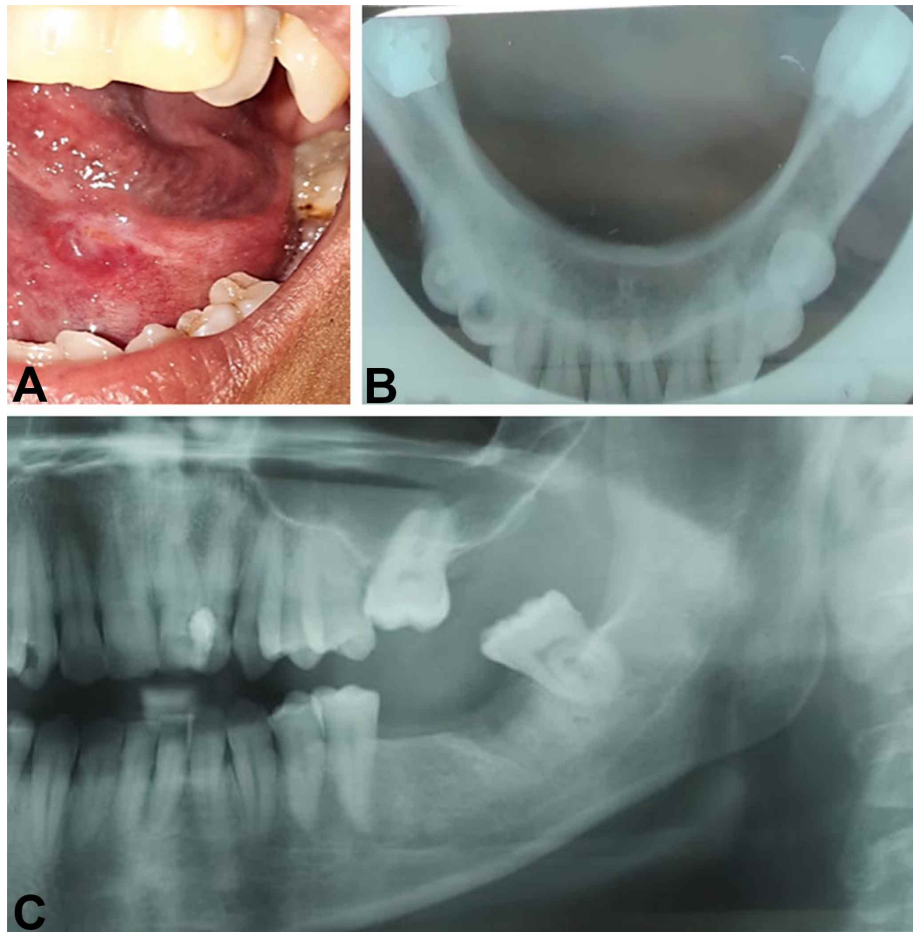


Fig. 1. Initial condition of the patient. Ranula lesion with increased volume on the floor of the mouth and central vitreous color. A. After analyzing the occlusal. B. and panoramic; C. radiographs, the presence of sialoliths correlated with the lesion was not identified.

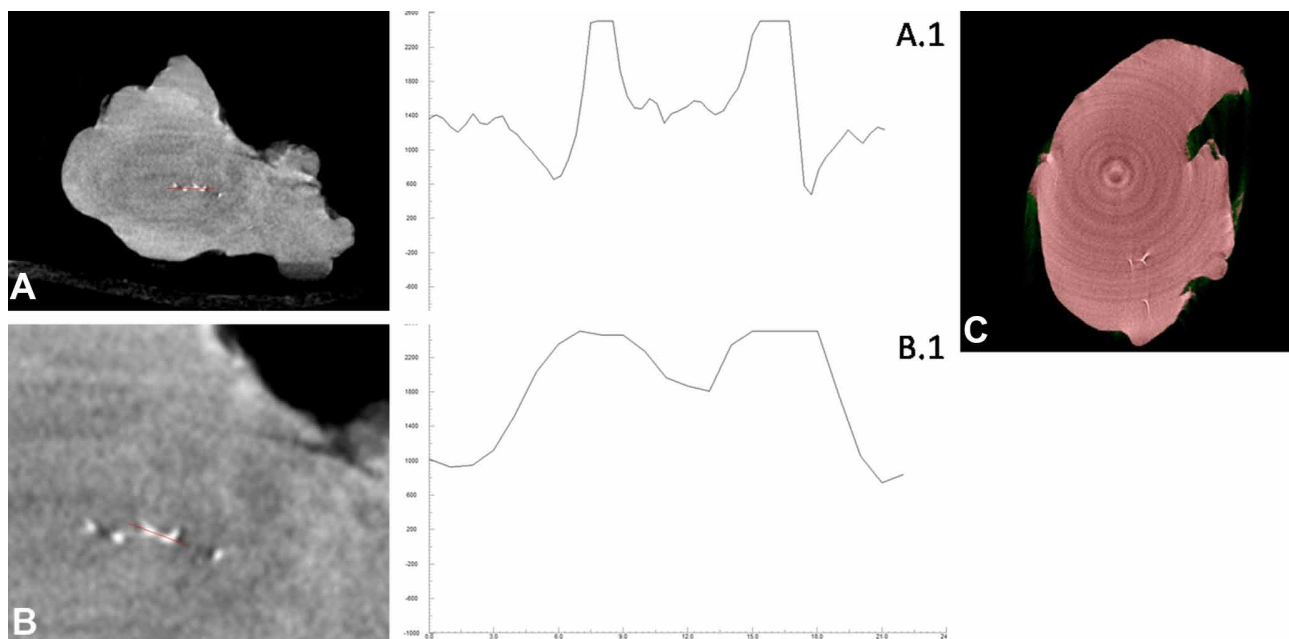


Fig. 2. Histomorphological analysis without contrast agent. A. Identification of sialoliths inside the biopsied fragment. B. areas of calcification through the Hounsfield unit (red line). Graphic representation of the Hounsfield unit in areas suggestive of calcification sialoliths (A.2 and B.2) using the Data Viewer software. Analysis in Ctan software, with binarization (C) revealing the sialoliths.

in the biopsied piece, in the second moment of impregnation in 2 % Elemental Iodine solution, led to a reduction of the HU, between -30 and -220 the regions suggestive of sialoliths, while the surrounding tissue areas were between -410 and -560 HU. The reduction of the filter at the time of image acquisition suggested the occurrence of a reduction in the contrast effect of the image representing a reduction

in the HU in the composition of the images of the biopsy specimen, since this unit is directly dependent on the contrast effect of the images.

However, it was possible to observe the same pattern of differentiation between tissue area and calcified areas of sialoliths, allowing their identification.

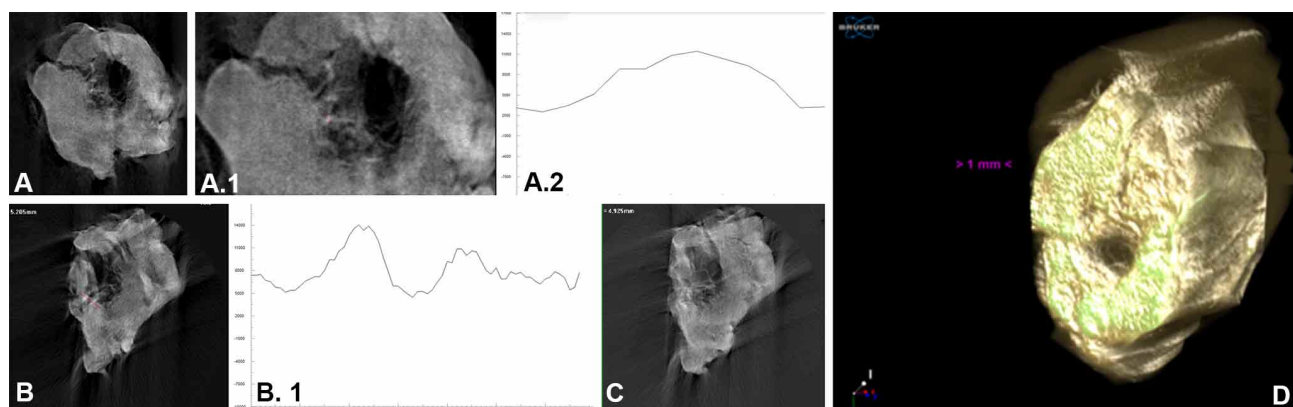


Fig. 3. Histomorphological analysis with a contrast agent using a 0.25 aluminum filter. Analysis using the Data Viewer software: Image suggestive of glandular duct with sialoliths dispersed inside (Imag. A and B) with the identification of sialoliths inside the salivary duct, indicating calcification through the Hounsfield unit (red line) (Imag. A.1 and B, red line). Graphic representation of the Hounsfield unit in areas suggestive of sialoliths (Imag. A.2 and B.1). Analysis in the Ctan software (Imag.C) revealed the less evident sialoliths in relation to the surrounding tissue, revealing a greater absorption of the tissues by the contrasting agent. 3D analysis on CtVox demonstrating the salivary duct of the biopsy specimen (Imag. D).

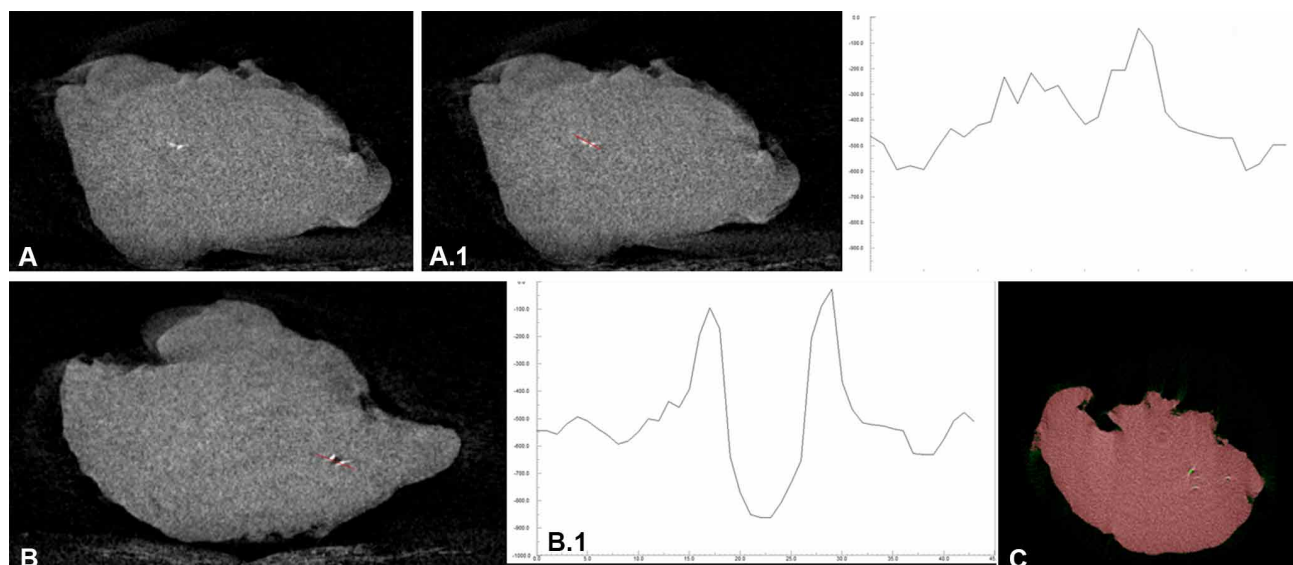


Fig. 4. Histomorphological analysis with contrast agent and 0.0 aluminum filter. Analysis through the Data Viewer software: sialoliths dispersed in its interior (Imag.A and B). Identification of sialoliths indicating calcification through the Hounsfield unit (red line) (Imag. A.1 and B, red line). Indicating peaks in the Hounsfield unit in areas suggestive of sialoliths (Imag. A.2 and B.1). Analysis in Ctan software (Imag.C) revealing the sialoliths.

## DISCUSSION

Computed tomography makes it possible to reconstruct the analyzed object in a 3D image. For the differentiation of internal microstructures to occur, there must be a partial absorption of the x-rays of the  $\mu$ Ct system in a heterogeneous way. A partial absorption of X-rays throughout the analyzed object, in a homogeneous way, will generate images of uniform shades of gray. Therefore, ideally, differential absorption occurs, with different parts of the object having significantly different x-ray absorption (Metscher, 2009). The use of contrast agents made this differential X-ray absorption relationship possible, as demonstrated in the acquisition of projection images, achieving a better contrast, and evidencing the glandular duct, during the analysis of the biopsied material, when impregnated with Elemental iodine solution at 2 %. Matos *et al.* (2020) also used  $\mu$ Ct scanning and image analysis systems for cardiopathology studies in a feline model using iodine labeling, making it possible to differentiate the types of cardiac tissues based on the differential attenuation of x-rays. The authors also point out the relevance, for obtaining the results, of the fact that  $\mu$ Ct provides 3D virtual plans of the whole heart, thus allowing a complete cardiac assessment. The  $\mu$ Ct would be especially useful in conditions where the lesions are irregularly distributed, increasing the precision in the histomorphological analyses, also making it possible to form image banks for histological studies (Matos *et al.*, 2020).

Until recently, quantitative histological techniques were the standards for assessing the architecture of bone samples. Although histological analyzes provide unique information about cellularity and bone remodeling indices, such analyzes have limitations regarding the assessment of bone microarchitecture, because the parameters used in these analyzes are derived from a histological slide that results from 2D sections (Bouxsein *et al.*, 2010). As for bone samples,  $\mu$ Ct may represent an advance in the histopathological study of tissue lesions. Methods for obtaining 2D images are well standardized, having high resolution, however, they demand time and skillful effort for the previous preparation of the samples. In another way,  $\mu$ Ct has been used for morphopathological analyses, such as arthritis and osteoporosis, allowing quantitative and qualitative characterization through parameters extracted during image processing (Amanai *et al.*, 2008).

On the other hand, Bouxsein *et al.* (2010) emphasized the need to standardize terminology, units and the set of minimum variables that must be reported in studies involving  $\mu$ Ct in the ex vivo analysis of species. The authors emphasized that information such as scanning aspects including scanning medium, x-ray tube potential and voxel size should be included. In image processing, the image filtering algorithm and segmentation approaches should be reported. A methodology similar to this proposal was made by Amanai *et al.* (2008), when performing ex vivo analyzes of mice with osteoarthritis induced by *Candida albicans*. The researchers detailed the scanning patterns, with the 45 kV and 48  $\mu$ A x-ray system and 3 to 5 mm scan, and the analysis of the images obtained, with a 3D structural analysis software – TRI/3D BON.

Adjusting the scanning parameters to obtain quality projection images for correct evaluation is an important part of the histomorphological analysis process using  $\mu$ Ct. The reduction of the Aluminum filter from 0.25 to 0.0 represented a loss of quality in the projection images leading to an increase in noise and loss of contrast in the biopsy specimen when impregnated with 2 % Elemental Iodine solution. The use of the filter will reduce the beam hardening effect, which is the incident x-ray energy spectrum that changes as it passes through the sample, the use of the filter will reduce this energy spectrum (Bouxsein *et al.*, 2010).

Filtering is determined by materials with different thicknesses, such as aluminum (Al), being used to reduce x-ray spectrum artifacts, attenuating the radioactive flux, removing those that are of low energy absorbed by the beam (Orhan, 2020). However, filtering needs attention regarding its use, as it decreases the image contrast and increases the signal-to-noise ratio (Orhan, 2020). Meganck *et al.* (2009) reported a direct relationship of increased filtration with reduced low energy levels, where there are two related criteria for filter smoothing, the first is sigma, which indicates the variation of the voxel gray scale mean, and the second is the support that represents the width in pixels or voxels that the smoothing is applied to. Hamba *et al.* (2012), showed that aluminum and copper filters together decrease image artifacts, even without using beam-hardening correction (BHC) afterwards.

As in our report, different studies have reported the use of different contrasting agents. Debbaut *et al.* (2014) studied human hepatic vascular organization by applying resin contrast to the hepatic artery and

portal vein when scanned in  $\mu$ Ct. The association of resin contrast during the scan allowed a detailed assessment of the macrocirculation and mesocirculation of this organ. In sequence, Missbach-Guentener *et al.* (2018), in order to perform a 3D virtual histological observation in animal models with  $\mu$ Ct renal lesions, used phosphotungstic acid as a method of *ex vivo* staining of the pieces, where their structural aspects could be visualized with adequate contrast, such as vessels, medulla, renal pelvis and other areas, thus showing that its staining method associated with  $\mu$ Ct contributed to the findings caused by this disease. Castro *et al.* (2018), reported the applicability of  $\mu$ Ct in histopathological studies, in the morphological characterization of peritoneal tube fistula and ectopic pregnancy, using impregnation with Lugol's iodide solution. Another methodology that can be pointed out for histopathological analysis was performed by Matos *et al.* (2020), when using 4 % sodium thiosulfate for 48 hours in order to remove iodine. Thus allowing the return of the samples for immersion in a 10 % formaldehyde solution to perform the histological sections with hematoxylin and eosin and Masson's trichrome.

Samples with higher atomic numbers, such as those obtained after impregnation in 2 % Elemental iodide solution, and with lower X-ray energy result in higher quality images. In their work, Matos *et al.* (2020) pointed through  $\mu$ Ct the existence of a replacement fibrosis, such as hypodense areas, in the feline heart. These investigators believe that iodine improved myocardial contrast in post-mortem species by being immobilized within myocyte glycogen, causing greater attenuation of x-rays in the myocardium than in fibrous tissue, which is then seen in  $\mu$ Ct as hyperdense areas. Previously, Metscher (2009) used the histogram as a parameter for a quantitative evaluation of contrast in  $\mu$ CT of samples impregnated with different contrast agents, inorganic iodine and phosphotungstic acid, concluding that these agents produce a differential contrast of the tissues. The evaluation by the Hounsfield unit is not far from the work presented here, since this unit is also defined by the intensity of the pixels, defined by the contrast of the image. Bouxsein *et al.* (2010) reported that scan results can be reported in terms of pixel brightness using Hounsfield units or the linear attenuation coefficient. The grayscale voxel values can be analyzed as a modality in order to obtain a correlation of absorption of the contrast agent in the sample for a given spectrum of x-ray beam (Metscher, 2009).

Artifacts such as noise and smudges can impair object segmentation, and can be reduced by increasing the image signal strength, while Ring artifacts arise from the incremental rotation of the object-camera, during image acquisition, in association with the non-uniformity of x-ray detection, as indicated in the analysis of the biopsy specimen without the use of the contrast agent. However, the use of the contrast agent, Elemental Iodine solution at 2 %, associated with increasing the exposure time from 4000 ms to 5200 ms, achieved this uniformity in the piece, eliminating this type of artifact when comparing the first analysis, of the biopsied piece, immersed in 10 % formalin solution with the piece impregnated with 2 % elemental iodine solution.

Limitations of contrast agents are related to the ability of the staining agent to diffuse into the samples and the need for prolonged exposure to the contrast agent for staining to occur. When used in high concentrations, these contrast agents can cause tissue shrinkage while low concentrations can limit the range of the contrast agent (Orhan, 2020). The concentration of 2 % of Elemental iodine solution indicated a homogeneity in this impregnation process, throughout the sample, visually verified in the Ctan and DataViewer software.

The method presented here can be used for an initial histopathological evaluation, as demonstrated. However, the visualization of structures, such as the glandular duct, was only possible with the use of the contrast agent, being indicated to improve the contrast of 3D tissue samples (Orhan, 2020).

## CONCLUSION

The comparison between the 3D images with and without a specific marker highlighted a better evidencing of the soft tissues, with an improvement in the contrast of the images, also allowing the identification of the glandular duct obstructed by the sialoliths, allowing a conclusive histopathological evaluation of the biopsy lesion. The 2 % Elemental Iodine solution enabled an improvement in the resolution of 3D images, providing a possibility for non-destructive histopathological evaluation of surgical specimens, and it was also possible to differentiate calcified areas from soft tissue areas through the use of the Hounsfield unit.

**ACKNOWLEDGMENTS.** This work was supported by Funadesp and Foundation for Research Financial Support in the State of Rio de Janeiro (FAPERJ).

**DOS SANTOS, E.; VIEIRA, W. C.; HEGGENDORN, F. L.** Evaluación patológica por microtomografía de rânula - reporte de caso clínico. *Int. J. Odontostomat.*, 16(2):214-221, 2022.

**RESUMEN:** Este estudio tiene como objetivo demostrar, a través de un reporte de caso clínico, la aplicabilidad del uso de la microtomografía ( $\mu$ CT) en la evaluación histopatológica de una lesión de rânula en el piso de la cavidad oral y evaluar el uso de solución de yodo elemental al 2 % como agente de contraste, con el fin de obtener un mejor efecto de contraste en una muestra de tejido, facilitando así la identificación de estructuras anatómicas, la evaluación histomorfológica y el potencial uso de  $\mu$ CT en el diagnóstico por imágenes de lesiones. Se evaluaron diferentes parámetros para la obtención de imágenes en SkyScan 1172, en una pieza biopsiada, cuando se impregna en una solución de formalina al 10 % y en una solución de yodo elemental al 2 %, durante 24 h y 48 h. La impregnación del agente de contraste se evaluó utilizando la unidad Hounsfield. El uso de  $\mu$ CT permitió la identificación de sialolitos dispersos dentro de la muestra de la biopsia, mientras que la impregnación con Yodo Elemental al 2 % durante 24 h resultó en un mejor contraste en comparación con las otras condiciones. El uso de la unidad Hounsfield permitió una adecuada evaluación del contraste obtenido cuando se aplicaron los diferentes parámetros de impregnación y adquisición de imágenes. La comparación entre las imágenes 3D con y sin marcador específico destacó una mejor evidenciación de los tejidos blandos, con una mejora en el contraste de las imágenes, permitiendo además identificar el conducto glandular obstruido por los sialolitos, permitiendo una evaluación histopatológica concluyente de la lesión sometida a biopsia.

**PALABRAS CLAVE:** rânula, microtomografía de rayos X, impregnación.

## REFERENCES

- Amanai, T.; Nakamura, Y. S.; Aoki, S. & Mataga, I. Micro-CT analysis of experimental Candida osteoarthritis in rats. *Mycopathologia*, 166(3):133-41, 2008.
- Bouxein, M. L.; Boyd, S. K.; Christiansen, B. A.; Guldberg, R. E.; Jepsen, K. J. & Müller, R. Guidelines for assessment of bone microstructure in rodents using micro-computed tomography. *J. Bone Miner. Res.*, 25(7):1468-86, 2010.
- Castro, P. T.; Matos, A. P. P.; Aranda, O. L.; Marchiori, E.; Alves, H. D. L.; Machado, A. S.; Lopes, R. T.; Werner, H. & Júnior, E. A. Tuboperitoneal fistula, ectopic pregnancy, and remnants of fallopian tube: a confocal microtomography analysis and 3D reconstruction of human fallopian tube pathologies. *J. Matern. Fetal Neonatal Med.*, 32(18):3082-7, 2018.
- Debbaut, C.; Segers, P.; Cornillie, P.; Casteleyn, C.; Dierick, M.; Laleman, W. & Monbaliu, D. Analyzing the human liver vascular architecture by combining vascular corrosion casting and micro-CT scanning: a feasibility study. *J. Anat.*, 224(4):509-17, 2014.
- Gomes, F. P.; Perciano, I. C. A.; Oliveira, D. M.; Santos, B. T. M.; Canuto, L. C.; Oliveira, A. L. P. & Peixoto, F. B. Técnica de marsupialização em rânula: relato de caso. *Rev. Electron. Acesso Saúde*, 37(37):e2369, 2019.
- Hamba, H.; Nikaido, T.; Sadr, A.; Nakashima, S. & Tagami, J. Enamel lesion parameter correlations between polychromatic microCT and TMR. *J. Dent. Res.*, 91(6):586-91, 2012.
- Heimel, P.; Swiadek, N. V.; Slezak, P.; Kerbl, M.; Schneider, C.; Nußmberger, S.; Redl, H.; Teuschl, A. H. & Hercher, D. Iodine-enhanced micro-CT imaging of soft tissue on the example of peripheral nerve regeneration. *Contrast Media Mol. Imaging*, 2019:7483745, 2019.
- Manzi, F. R.; Silva, A. I.; Dias, F. G. & Ferreira, E. F. Sialolito na Glândula Submandibular: Relato de caso clínico. *Rev. Odontol. Bras. Cent.*, 19(50):270-4, 2010.
- Matos, J. N.; Canadilla, P. G.; Simcock, I. C.; Hutchinson, J. C.; Dobromylskyj, M.; Guy, A.; Arthurs, O. J.; Cook, A. C. & Fuentes, V. L. Micro-computed tomography (micro-CT) for the assessment of myocardial disarray, fibrosis and ventricular mass in a feline model of hypertrophic cardiomyopathy. *Sci. Rep.*, 10:20169, 2020.
- Meganck, J. A.; Kozloff, K. M.; Thornton, M. M.; Broski, S. M. & Goldstein, S. A. Beam hardening artifacts in microcomputed tomography scanning can be reduced by X-ray beam filtration and the resulting images can be used to accurately measure BMD. *Bone*, 45(6):1104-16, 2009.
- Metscher, B. D. MicroCT for developmental biology: a versatile tool for high-contrast 3D imaging at histological resolutions. *Dev. Dyn.*, 238(3):632-40, 2009.
- Missbach-Guentener, J.; Leetsch, D. P.; Dullin, C.; Ufartes, R.; Hornung, D.; Tampe, B.; Zeisberg, M. & Alves, F. 3D Virtual histology of murine kidneys – high resolution visualization of pathological alterations by micro computed tomography. *Sci. Rep.*, 8:1407, 2018.
- Mizuno, A. & Yamaguchi, K. The plugging ranula. *Int. J. Oral Maxillofac. Surg.*, 22(2):113-5, 1993.
- Neville, B. W.; Damm, D. D. & Allen, C. M. *Patologia Oral e Maxilofacial*. 4th ed. Rio de Janeiro, Elsevier, 2016.
- Orhan, K. *Micro-computed Tomography (micro-CT) in Medicine and Engineering*. Istanbul, Springer, 2020.
- Peyrin, F.; Dong, P.; Pacureanu, A. & Langer, M. Micro- and nano CT for the study of bone ultrastructure. *Curr. Osteoporos. Rep.*, 12(4):465-74, 2014.
- Queiroz, P. J. B.; Silva, A. K. M.; Freitas, S. L. R.; Assis, B. M. & Silva, L. A. F. Microtomografia Computadorizada: Princípios de funcionamento e utilização em amostras biológicas. *Encicl. Biosf.*, 16(29):1073, 2019.
- Corresponding author:  
Fabiano Luiz Heggendorn.  
Postgraduate Program in Dentistry  
University of Grande Rio (UNIGRANRIO)  
Rua Prof. José de Souza Herdy, 1160 block C  
2nd floor – August 25th  
Duque de Caxias / Rio de Janeiro  
BRAZIL
- E-mail: fabianohegg@gmail.com
- Ellen dos Santos. orcid:0000-0002-3319-4994  
Walas Cazassa Vieira. orcid: 0000-0003-2538-4437  
Fabiano Luiz Heggendorn. orcid:0000-0002-2687-0165